



ELSEVIER

Contents lists available at ScienceDirect

Journal of Sound and Vibration

journal homepage: www.elsevier.com/locate/jsvi

A hierarchy of dynamic equations for micropolar plates



Hossein Abadikhah, Peter D. Folkow*

Department of Applied Mechanics, Chalmers University of Technology, SE-412 96 Göteborg, Sweden

ARTICLE INFO

Article history:

Received 3 March 2015

Received in revised form

4 August 2015

Accepted 5 August 2015

Handling Editor: S. Ilanko

Available online 21 August 2015

ABSTRACT

This work considers homogeneous isotropic micropolar plates adopting a power series expansion method in the thickness coordinate. Variationally consistent equations of motion and end boundary conditions are derived in a systematic fashion up to arbitrary order for extensional and flexural displacement cases. The plate equations are asymptotically correct to all studied orders. Numerical results are presented for various orders of the present method, other approximate theories as well as the exact three dimensional theory. The results illustrate that the present approach may render benchmark solutions provided higher order truncations are used, and act as engineering plate equations using low order truncation.

© 2015 The Authors. Published by Elsevier Ltd. This is an open access article under the CC BY-NC-ND license (<http://creativecommons.org/licenses/by-nc-nd/4.0/>).

1. Introduction

Micropolar elasticity introduces dependency on the microstructure of a continuum within the framework of classical continuum theory. Extending the classical continuum model is relevant for materials where internal or microscale characteristics drastically alters the response behavior. Such materials can range from granular to fibrous material and even composites can fall under the category of micropolar theory, since microstructure defines mechanical properties. Hence, micropolar elasticity theory is an extension of classical elasticity theory. This extension entails that, unlike classical elasticity theory where only three translational degrees of freedom are assigned to each material point within a body; micropolar elasticity theory also introduces three rotational degrees of freedom to each material point. In effect, each material point is considered to be a rigid body. As a consequence, two types of stresses are experienced by a material point during external loading, the extension of the Cauchy stress in micropolar elasticity theory and a new stress denoted couple stress. Both these stresses are in the general case nonsymmetric.

Since the development of the micropolar theory due to Cosserat [1] several alternative versions have evolved, most notably the theory by Eringen [2]. There exists many works where micropolar theories have been applied to structure elements such as for plates, see for example the review paper by Altenbach et al. [3]. Among these works, the study of Kirchhoff and Mindlin type plate theories has been developed by several authors [4–13]. In addition, different types of micropolar plate equations based on asymptotic expansion theories have been studied by Green and Naghdi [5], Achenbach [14] and Erbay [15].

The purpose of the present work is to derive a hierarchy of theories for plates based on the micropolar continuum theory developed by Eringen [2]. This results in plate equations and pertinent sets of edge conditions developed in a consistent and systematic fashion up to arbitrary order. The present approach differs to the previous work on approximate micropolar plate

* Corresponding author. Tel.: +46 31 7721521; fax: +46 31 772 3827.

E-mail addresses: hossein.abadikhah@chalmers.se (H. Abadikhah), peter.folkow@chalmers.se (P.D. Folkow).

theories in several important ways such as the series expansion procedure, the way of collecting terms and the truncation process as a whole. The used method is mainly based on the works on isotropic plates by Boström et al. [16] and anisotropic plates by Mauritsson et al. [17]. This particular method has also been employed for functionally graded plates [18], porous plates [19], shells [20], rods [21,22] and beams [23].

In short, the present plate equations for homogenous isotropic micropolar plates are derived by employing a systematic power series expansion approach. Displacement and micro-rotation fields are expanded in a power series in the thickness coordinate of the plate. From the expanded displacements and micro-rotations, the stress and couple stress are obtained on power series form in terms of the expansion functions of the displacements and micro-rotations. Furthermore, by using the equations of motion for micropolar elasticity, recursion relations are constructed. These are used to express all expansion functions in terms of the lowest order expansion functions. Thus all fields can be expressed in these lowest order expansion functions without performing any truncations. Subsequently boundary conditions on the upper and lower surface of the plate are stated on power series form. These boundary conditions represent a set of scalar equations, written in terms of the lowest order expansion functions. The scalar equations constitute the complete set of partial differential plate equations for extensional and flexural motion, which may also be decoupled if necessary. Using variational calculus, the edge boundary conditions for each edge surface are obtained in an equally systematic manner. The resulting sets of plate equations may be truncated to any order, where each studied order is asymptotically correct.

In order to validate the hierarchy of plate theories, numerical results for dispersion curves, eigenfrequencies and cross sectional fields are presented using different truncation orders. Comparisons are made to the exact three dimensional theory as well as to the approximate theories due to Eringen [4] and Sargsyan and Sargsyan [10].

2. Theory of linear micropolar elasticity

Consider a micropolar continuum where the field variables are expressed in Cartesian coordinates. In the absence of body forces and body couples, the equations of balance of momentum and moment of momentum are written as [2]

$$t_{kl,k} = \rho \ddot{u}_l, \quad (1)$$

$$m_{kl,k} + \epsilon_{lkm} t_{km} = \rho j_{lk} \ddot{\phi}_k, \quad (2)$$

where t_{kl} is the stress tensor, m_{kl} is the couple stress tensor, u_l is the displacement vector, ϕ_k is the micro-rotation vector, ρ is the density, j_{lk} is the microinertia tensor and ϵ_{lkm} is the permutation symbol. Indices that follow a comma indicate partial differentiation. The tractions are defined in accordance to

$$t_l = t_{kl} n_k, \quad (3)$$

$$m_l = m_{kl} n_k, \quad (4)$$

where n_k is an outward pointing normal.

Supplementing the equations of motion, two constitutive relations for the stress and couple stress are needed. For a homogenous and isotropic material the constitutive relations are given by

$$t_{kl} = \lambda \epsilon_{mm} \delta_{kl} + (\mu + \kappa) \epsilon_{kl} + \mu \epsilon_{lk}, \quad (5)$$

$$m_{kl} = \alpha \gamma_{mm} \delta_{kl} + \beta \gamma_{kl} + \gamma \gamma_{lk}, \quad (6)$$

where δ_{kl} is the Kronecker delta, λ and μ are Lamé parameters while α , β , γ and κ are micropolar elastic moduli. For spin-isotropic materials the microinertia reduces to a scalar quantity, $j_{kl} = j \delta_{kl}$. Moreover the micropolar strain tensors ϵ_{kl} and γ_{kl} are defined by

$$\epsilon_{kl} = u_{l,k} + \epsilon_{lkm} \phi_m, \quad (7)$$

$$\gamma_{kl} = \phi_{k,l}. \quad (8)$$

3. Series expansion and recursion relations

The governing equations for a micropolar continuum as described in Section 2 are to be applied to a homogenous isotropic plate of thickness $2h$. A Cartesian coordinate system $\{x, y, z\}$ is used, where the in plane x - and y -axes are along the middle plate plane at $z=0$. The components of the displacement field and micro-rotation field are denoted $\{u_1, u_2, u_3\}$ and $\{\phi_1, \phi_2, \phi_3\}$ respectively. The derivation procedure of the plate equations is based on the assumption that each component of the displacement field and micro-rotation field can be expanded in a power series in the thickness coordinate z according to

$$u_i(x, y, z, t) = \sum_{n=0}^{\infty} z^n u_i^{(n)}(x, y, t), \quad (9)$$

$$\phi_l(x, y, z, t) = \sum_{n=0}^{\infty} z^n \phi_l^{(n)}(x, y, t). \tag{10}$$

Before proceeding with the derivation of the plate equations, an operator L_k is defined to simplify calculations. L_k operates on the displacement and micro-rotation fields in the following manner:

$$L_k f_l^{(n)} = \begin{cases} \partial_x f_l^{(n)} & \text{if } k = 1, \\ \partial_y f_l^{(n)} & \text{if } k = 2, \\ (n+1) f_l^{(n+1)} & \text{if } k = 3, \end{cases} \tag{11}$$

i.e. L_k for $k=3$ increases the index of $f_l^{(n)}$ and multiplies with the new index, in this case $n+1$. Here the shorthand form ∂_x and ∂_y are used to denote partial derivatives with respect to x and y . Using the assumptions in Eqs. (9) and (10), the constitutive equations (5) and (6), as well as the deformation relation equations (7) and (8), it is possible to express all the stress and couple stress components in power series form

$$t_{kl} = \sum_{n=0}^{\infty} z^n t_{kl}^{(n)}, \tag{12}$$

$$m_{kl} = \sum_{n=0}^{\infty} z^n m_{kl}^{(n)}, \tag{13}$$

where

$$t_{kl}^{(n)} = \lambda L_i u_i^{(n)} \delta_{kl} + \mu (L_i u_k^{(n)} + L_k u_i^{(n)}) + \kappa (L_k u_l^{(n)} + \epsilon_{lkm} \phi_m^{(n)}), \tag{14}$$

$$m_{kl}^{(n)} = \alpha L_i \phi_i^{(n)} \delta_{kl} + \beta L_i \phi_k^{(n)} + \gamma L_k \phi_l^{(n)}. \tag{15}$$

By inserting the expanded displacement and micro-rotation fields (Eqs. (9) and (10)), together with the expanded stress and couple stress tensors (Eqs. (12) and (13)) into the equations of motion, Eqs. (1) and (2), and collecting terms of equal power in z one can obtain recursion formulas for each displacement and micro-rotation field. The recursion formulas are essential for the derivation of the plate equations since the number of expansion functions for each field can be reduced from an infinite amount to a finite amount. By using the recursion formulas it is possible to express all expansion functions $u_l^{(n)}$ and $\phi_l^{(n)}$ with $n = \{2, 3, \dots\}$ in terms of the lowest order ones with $n = \{0, 1\}$. The recursion formulas are obtained as

$$\begin{aligned} & (\mu + \kappa)(n+2)(n+1)u_l^{(n+2)} + (\lambda + \mu)(n+2)(n+1)u_3^{(n+2)}\delta_{3l} \\ & = \rho \ddot{u}_l^{(n)} - (\mu + \kappa)(\partial_x^2 + \partial_y^2)u_l^{(n)} - (\lambda + \mu)L_i(\partial_x u_1^{(n)} + \partial_y u_2^{(n)}) \\ & \quad + (n+1)u_3^{(n+1)}(1 - \delta_{3l}) - \kappa \delta_{li} \epsilon_{ijk} L_j \phi_k^{(n)}, \quad n = 0, 1, \dots, \end{aligned} \tag{16}$$

$$\begin{aligned} & \gamma(n+2)(n+1)\phi_l^{(n+2)} + (\alpha + \beta)(n+2)(n+1)\phi_3^{(n+2)}\delta_{3l} \\ & = \rho j \ddot{\phi}_l^{(n)} - \gamma(\partial_x^2 + \partial_y^2)\phi_l^{(n)} - (\alpha + \beta)L_i(\partial_x \phi_1^{(n)} + \partial_y \phi_2^{(n)}) \\ & \quad + (n+1)\phi_3^{(n+1)}(1 - \delta_{3l}) - \kappa(\delta_{li} \epsilon_{ijk} L_j u_k^{(n)} - 2\phi_l^{(n)}), \quad n = 0, 1, \dots, \end{aligned} \tag{17}$$

for $l=1, 2, 3$. Note that these coupled six recursion formulas do not involve any approximations since they stem from the equations of motion, Eqs. (1) and (2), and the power series expansion of the displacement and micro-rotation fields, Eqs. (9) and (10). Furthermore, the power series have not been truncated which is essential for the present method.

4. Dynamic plate equations

On the surfaces at $z = \pm h$, either the tractions or the displacements and micro-rotation are to be prescribed. These given fields are denoted $\{T_l^\pm, M_l^\pm, U_l^\pm, \Phi_l^\pm\}$, where \pm indicates the upper surface $z=h$ and the lower surface $z=-h$, respectively. Hence one field from each pair $\{t_{3l}, u_l\}$ and $\{m_{3l}, \phi_l\}$ is prescribed, resulting in six boundary conditions for each surface. For prescribed stresses, the boundary condition is obtained by truncating Eqs. (12) and (13) at an order $N > 0$, which gives

$$\sum_{n=0}^N (\pm h)^n t_{3l}^{(n)}(x, y, t) = T_l^\pm(x, y, t), \quad \sum_{n=0}^N (\pm h)^n m_{3l}^{(n)}(x, y, t) = M_l^\pm(x, y, t). \tag{18}$$

Similarly boundary conditions for displacements and micro-rotations are obtained from Eqs. (9) and (10),

$$\sum_{n=0}^{N+1} (\pm h) u_l^{(n)}(x, y, t) = U_l^\pm(x, y, t), \quad \sum_{n=0}^{N+1} (\pm h) \phi_l^{(n)}(x, y, t) = \Phi_l^\pm(x, y, t). \tag{19}$$

The conditions for the displacements and micro-rotations are truncated at a one order higher compared to the stresses. This is due to that stresses include spatial derivatives of one order higher than displacements and micro-rotations, therefore an extra term is added to these latter conditions in order to obtain consistent plate equations.

The boundary conditions obtained from combinations of Eqs. (18) and (19) constitute the hyperbolic set of twelve partial differential equations for a micropolar plate. Using the recursion relations, Eqs. (16) and (17), these plate equations may be written in terms of the twelve lowest order expansion functions $\{u_i^{(n)}, \phi_i^{(n)}\}$ for $n = \{0, 1\}$. These surface boundary conditions are always fulfilled regardless of the expansion order N . Each of the twelve boundary conditions, Eqs. (18) and (19), contain spatial derivatives of order $N+1$ for $\{u_i^{(0)}, \phi_i^{(0)}\}$ and spatial derivatives of order N for $\{u_i^{(1)}, \phi_i^{(1)}\}$. Although any combination of boundary conditions may be treated, consider from here on plates where either only tractions or only displacements and micro-rotations are prescribed at the surfaces $z = \pm h$. Hereby, the resulting system of twelve plate equations will have a differential order of $12N$. This is seen by reducing the twelve plate equations to a single equation in any of the scalar fields $\{u_i^{(n)}, \phi_i^{(n)}\}$ for $n = \{0, 1\}$. Consequently $6N$ boundary conditions must be selected for each edge of the plate.

In practice it is more convenient to decouple the plate equations into equations for symmetric motion and equations for antisymmetric motion. This is achieved by adding and subtracting the conditions, Eqs. (18) and (19), thereby obtaining conditions only containing even or odd expansions in h according to

$$\sum_{n \text{ even}}^N h^n t_{3l}^{(n)} = \frac{1}{2}(T_l^+ + T_l^-), \quad \sum_{n \text{ odd}}^N N h^n t_{3l}^{(n)} = \frac{1}{2}(T_l^+ - T_l^-), \quad (20)$$

$$\sum_{n \text{ even}}^N h^n m_{3l}^{(n)} = \frac{1}{2}(M_l^+ + M_l^-), \quad \sum_{n \text{ odd}}^N N h^n m_{3l}^{(n)} = \frac{1}{2}(M_l^+ - M_l^-), \quad (21)$$

$$\sum_{n \text{ even}}^{N+1} h^n u_l^{(n)} = \frac{1}{2}(U_l^+ + U_l^-), \quad \sum_{n \text{ odd}}^{N+1} N+1 h^n u_l^{(n)} = \frac{1}{2}(U_l^+ - U_l^-) \quad (22)$$

$$\sum_{n \text{ even}}^{N+1} h^n \phi_l^{(n)} = \frac{1}{2}(\Phi_l^+ + \Phi_l^-), \quad \sum_{n \text{ odd}}^{N+1} h^n \phi_l^{(n)} = \frac{1}{2}(\Phi_l^+ - \Phi_l^-), \quad (23)$$

Consequently for a plate where only tractions are prescribed at the surfaces $z = \pm h$, antisymmetric motion is obtained by selecting the first (even) sum of Eq. (20) for $l=1, 2$ and the second (odd) sum of Eq. (20) for $l=3$, as well as the second sum of Eq. (21) for $l=1, 2$ and the first sum of Eq. (21) for $l=3$. The complementary set is used for symmetric motion. For a plate where only displacements and micro-rotations are prescribed at the surfaces $z = \pm h$, the antisymmetric motion is obtained by selecting the second sum of Eqs. (22) for $l=1, 2$ and (23) for $l=3$, as well as the first sum of Eqs. (22) for $l=3$, and (23) for $l=1, 2$. Symmetric motion is obtained by using the complementary set. By adopting the recursion relations the antisymmetric motion only involves the six expansion functions $\{u_1^{(1)}, u_2^{(1)}, u_3^{(0)}, \phi_1^{(0)}, \phi_2^{(0)}, \phi_3^{(1)}\}$, while the symmetric motion involves the complementary set $\{u_1^{(0)}, u_2^{(0)}, u_3^{(1)}, \phi_1^{(1)}, \phi_2^{(1)}, \phi_3^{(0)}\}$. The decoupled plate equations are each of differential order $6N$, resulting in $3N$ boundary conditions along each edge of the plate.

Furthermore, these uncoupled set of plate equations may be analytically compared to the exact solution for infinite plates. By expanding the displacements and micro-rotations for some branch of the exact micropolar dispersion spectrum in a Taylor series around $z=0$, identical terms are obtained as from the present hyperbolic set for each studied truncation order N . Hence, this indicates that the present method renders asymptotically correct equations to arbitrary order N . Similar results are reported for flexural elastic plates [16,24] when using a series expansion approach. Note that odd N results in asymptotically correct equations to that specific order, while even N renders equations that are asymptotically correct to the nearest lower odd order [17]. Therefore only odd N are chosen in this work.

These sets of plate equations, Eqs. (20)–(23), may also be obtained using variational calculus. This is accomplished by following the general procedure illustrated in [22,23] adopting a generalized Hamilton's principle where stresses, couple stresses, displacements and micro-rotations are varied simultaneously and independently. In addition pertinent edge boundary is obtained in a variationally consistent manner as described below.

5. Edge conditions

Consider a rectangular plate where $-a \leq x \leq a$ and $-b \leq y \leq b$. At each edge $x = \pm a$ and $y = \pm b$ one field from each pair $\{t_{\alpha l}, u_l\}$ and $\{m_{\alpha l}, \phi_l\}$ is to be prescribed for all $z \in [-h, h]$, here $\alpha = \{1, 2\}$. The given fields are denoted $\{T_l^{\{\pm a, \pm b\}}, U_l^{\{\pm a, \pm b\}}\}$ and $\{M_l^{\{\pm a, \pm b\}}, \Phi_l^{\{\pm a, \pm b\}}\}$ for each edge. These prescribed edge boundary fields may be time dependent as well as having varying properties over the thickness and along each edge. The boundary conditions for each edge are constructed in a systematic manner by adopting a generalized Hamilton's principle [17,22,23]. Since all boundary conditions are constructed in the same manner, the procedure is only presented for a prescribed stress at $x=a$.

The variationally consistent edge boundary condition is then expressed as

$$\int_{-h}^h \left(T_l^{+a}(y, z, t) - \sum_{n=0}^M z^n t_{1l}^{(n)}(a, y, t) \right) z^k dz = 0, \quad k = 0, 1, \dots, M, \tag{24}$$

by using Eq. (12) and truncating at an order M . The $M+1$ integrals in Eq. (24) constitute a system of equations which solution renders the $M+1$ terms $t_{1l}^{(n)}(a, y, t)$ for $n = 0, 1, \dots, M$. This representation of the boundary condition in power series form is identical to the expansion of the given function T_l^{+a} in terms of Legendre polynomials $P_n(z/h)$ of order M , i.e.

$$T_l^{+a}(y, z, t) \approx \sum_{n=0}^M a_n(y, t) P_n(z/h) = \sum_{n=0}^M z^n T_l^{+a(n)}(y, t), \tag{25}$$

hence $t_{1l}^{(n)}(a, y, t) = T_l^{+a(n)}(y, t)$. Note that the stress free case $T_l^{+a} = 0$ results in $t_{1l}^{(n)} = 0$ for all n at the edge. By using Eq. (14) each edge boundary stress term $t_{1l}^{(n)}(a, y, t)$ is expressed in terms of displacements and micro-rotations. Adopting the recursions formulas, Eqs. (16) and (17), the boundary stresses are written as partial differential equations in terms of the lowest order fields $\{u_l^{(n)}, \phi_l^{(n)}\}$ for $n = \{0, 1\}$.

The prescribed edge fields are thus expanded in both even and odd powers of z in the general case, as indicated in Eq. (25). As noted before, the corresponding $6N$ edge conditions may be divided in $3N$ symmetric and $3N$ antisymmetric edge conditions using decoupled symmetric/antisymmetric plate equations.

6. Numerical results

The present micropolar partial differential plate equations using different truncation orders are to be studied numerically for the antisymmetric case with free upper and lower plate surfaces. This comprises investigating dispersion relations for time harmonic waves in a infinite plate and by investigating stress, displacement and micro-rotation distributions. Also, eigenfrequencies are calculated for finite square plates that are simply supported at all edges, as well as for two opposite edges that are simply supported and the other edges are clamped or free. All numerical results are compared with the approximate plate theories due to Eringen [4] and Sargsyan and Sargsyan [10] and when possible to the exact three dimensional theory. These approximate theories [4,10] mainly differ mutually concerning the micro-rotation around the axis perpendicular to the median plane. In Eringen's theory this degree of freedom is neglected while for Sargsyan's theory this quantity is varying linearly with respect to the thickness coordinate.

The studied plate material is aluminium, where the material parameters are $E=70.85$ GPa, $\nu=0.33$, $\rho = 2800$ kg/m³, $j = 0.325 \times 10^{-7}$, $\kappa = 1.31549 \times 10^{-5}$ GPa, $\alpha = 1.23552$ kN, $\beta = 0.1585$ kN, $\gamma = 0.59664$ kN [25]. Consider time harmonic conditions with the time factor $e^{-i\omega t}$ using the non-dimensional frequency $\Omega = \omega h/c_2$, where $c_2 = \sqrt{(\mu + \kappa)/\rho}$. Since only the antisymmetric case is studied, the lowest truncation of the plate equations is $N=3$ as the lower $N=1$ case does not correctly account for flexural effects. The used $N=3$ equations are presented in Appendix A.

6.1. Dispersion curves

Consider time harmonic waves propagating in the direction of the x -axis with wavenumber k . The first three flexural modes are obtained and compared between the theories. In Fig. 1 the three first modes are presented, where the non-dimensional frequency Ω is plotted against kh . For the present theory, the $N=3$, $N=5$ and $N=7$ truncations are used to effectively show the difference between truncations and the convergence of the solution to the exact theory.

The first curve, being the first flexural mode, is approximated quite well for small wavenumbers by all theories. The Sargsyan theory begins to divert from the exact solution at $kh \approx 0.7$, while the solutions of all other theories only degenerate slightly. The plate theory due to Eringen approximates the first flexural mode marginally better than the present $N=3$ theory while $N=5$ and $N=7$ are indistinguishable from the exact curve. For the second curve, the Sargsyan theory diverts at $kh \approx 0.1$, while the Eringen and $N=3$ theories render accurate approximations. Note that the Sargsyan solution for the

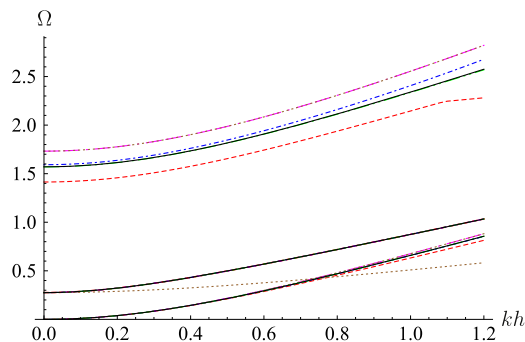


Fig. 1. Dispersion curves: — Exact, --- $N=3$, - · - $N=5$, · · · $N=7$, - - - Eringen, · · · Sargsyan.

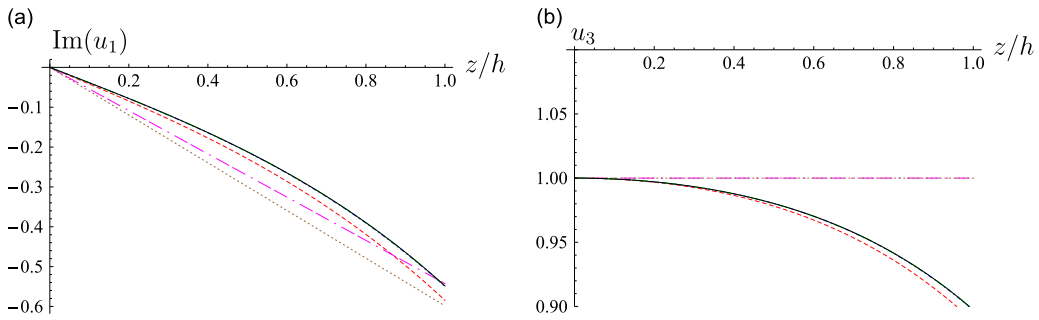


Fig. 2. Displacement in x -direction (b) and z -direction (a) for the first mode: — Exact, --- $N=3$, - - - $N=5$, - · - · - $N=7$, - - - - Eringen, · · · · Sargsyan.

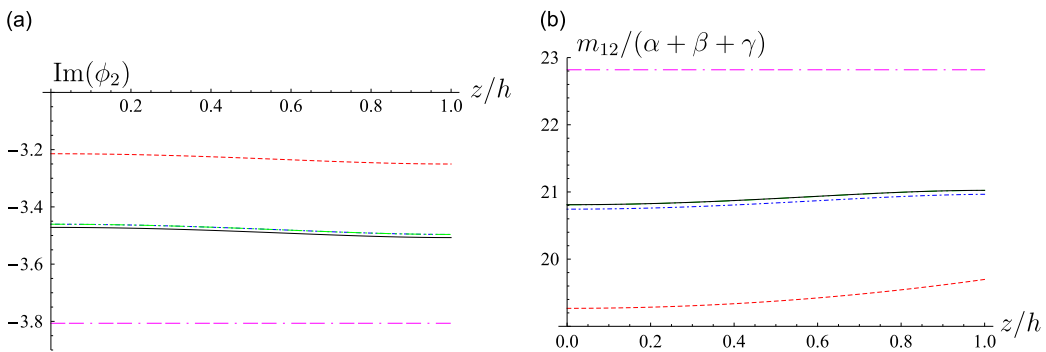


Fig. 3. Micro-rotation in y -direction (a) and couple stress m_{12} (b) for the first mode: — Exact, --- $N=3$, - - - $N=5$, - · - · - $N=7$, - - - - Eringen, · · · · Sargsyan.

second mode follows the curve of the first flexural mode for $kh \geq 0.7$, being on top of the Eringen curve. Concerning the third flexural mode, it is noted that Eringen's and Sargsyan's theories give the same solution, which results in a solution that is substantially larger than the exact solution. For the $N=3$ theory the opposite behavior is seen where the frequencies are lower than the exact solution and for $kh \approx 1.1$ the solution diverts from the exact theory. Note that at $kh \geq 1.1$ the fourth mode (not illustrated) continues along the path of the third mode for $kh \leq 1.1$, similar to the behavior of the Sargsyan solution of the first and second mode around $kh \approx 0.7$. Concerning the higher order approximations for the third mode, the $N=5$ theory is able to approximate the exact solution fairly accurately, although the approximation deteriorates as the wavenumber is increased, while the results for $N=7$ are indistinguishable from the exact curve.

6.2. Distributions over cross section

Consider a time harmonic wave traveling in the x -direction with the non-dimensional wavenumber $kh=1$, see Fig. 1. Here only the first and third mode are regarded, as the second mode behaves in a similar manner as the first mode. The obtained fields, stresses, couple stresses, displacements and micro-rotations are either real or imaginary, where the imaginary part is denoted by Im . Furthermore, all fields are either symmetric or antisymmetric with respect to the z -direction, hence only the upper half $0 \leq z \leq h$ is shown. Distributions are plotted as functions of the non-dimensional thickness coordinate z/h . To simplify comparisons between different theories, the fields are normalized so that the vertical displacement in the middle of the plate equals unity, $u_3(z=0) = 1$.

In Figs. 2–4 various fields are presented for the first mode. Fig. 2 shows the displacements in the x - and z -directions, u_1 and u_3 , respectively. Here the present $N=3$ theory renders superior results compared to Eringen and Sargsyan. Notice that for the displacement in the z -direction, Eringen's and Sargsyan's theories give a constant field and for the displacement in x -direction both these theories present a linear variation over the cross section. The results for $N=5$ and $N=7$ are indistinguishable from the exact solution. Fig. 3(a) and (b) presents the micro-rotation around the y -axis and the couple stress, respectively. Here Sargsyan's theory is not presented since this theory gives results that are unreasonably large compared to the exact solution. The present $N=3$ theory and Eringen's theory render approximations of the same modest accuracy, while the higher order theories $N=5$ and $N=7$ give superior results. In Fig. 3(b) the curve for the $N=7$ theory is indistinguishable from the exact solution. The normal and shear stress distributions are presented in Fig. 4, where the $N=3$ theory is superior compared to the linearly varying normal stresses and constant shear stresses according to Eringen and Sargsyan. The $N=5$ and $N=7$ theories are on top of the exact curve. Note that the present theory for all orders fulfills the boundary condition for the shear stress at the free surface in Fig. 4(b).

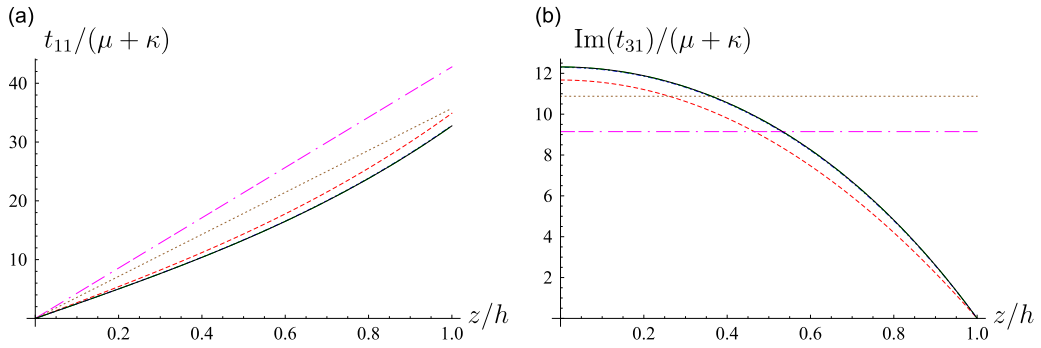


Fig. 4. Normal stress in x-direction (a) and stress t_{31} (b) for the first mode: — Exact, --- $N=3$, ···· $N=5$, - · - · $N=7$, - - - - Eringen, ···· Sargsyan.

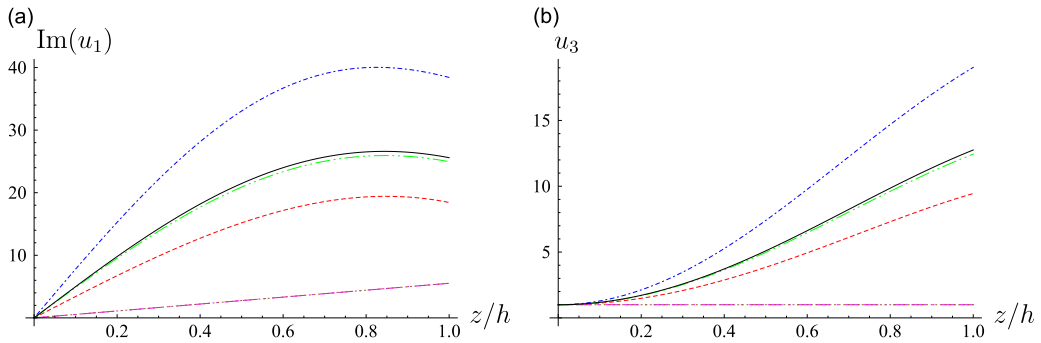


Fig. 5. Displacement in x-direction (a) and z-direction (b) for the third mode: — Exact, --- $N=3$, ···· $N=5$, - · - · $N=7$, - - - - Eringen, ···· Sargsyan.

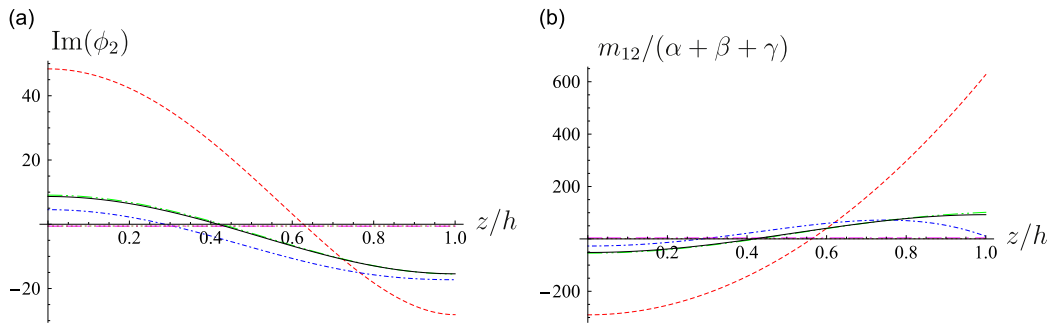


Fig. 6. Micro-rotation in y-direction (a) and couple stress m_{12} (b) for the third mode: — Exact, --- $N=3$, ···· $N=5$, - · - · $N=7$, - - - - Eringen, ···· Sargsyan.

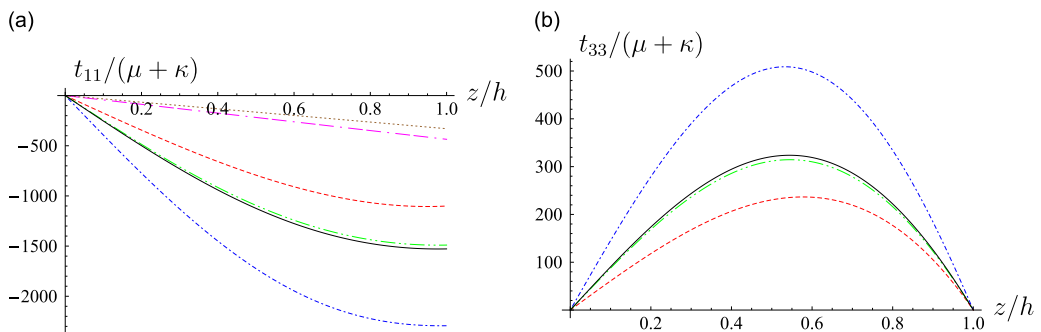


Fig. 7. Normal stress in x-direction (a) and normal stress in z-direction (b) for the third mode: — Exact, --- $N=3$, ···· $N=5$, - · - · $N=7$, - - - - Eringen, ···· Sargsyan.

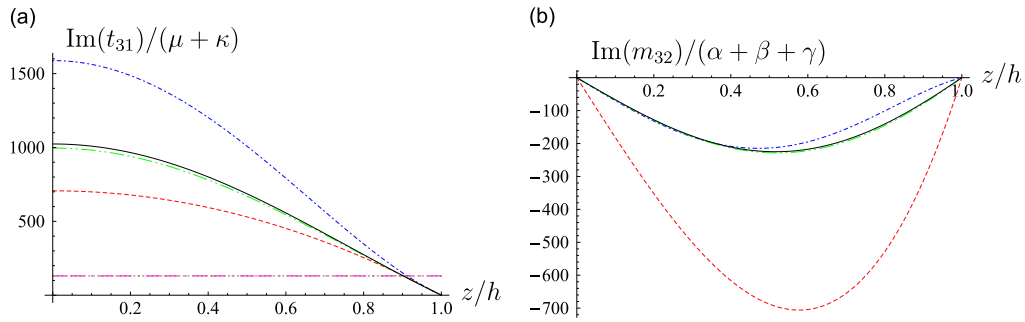


Fig. 8. Stress t_{31} (a) and couple stress m_{32} (b) for the third mode: — Exact, - - - $N=3$, · · · $N=5$, - · - · $N=7$, - - - - Eringen, · · · · Sargsyan.

Table 1

Simply supported plate: the eigenfrequencies Ω_{mn} for exact theory and the approximate theories: Eringen, Sargsyan, $N=3$, $N=5$, $N=7$ and $N=33$.

m	n	Exact	Eringen	Sargsyan	$N=3$	$N=5$	$N=7$	$N=33$
1	1	0.01220	0.01221	0.01221	0.01218	0.01220	0.01220	0.01220
2	1	0.03010	0.03016	0.03016	0.03001	0.03010	0.03010	0.03010
2	2	0.04756	0.04770	0.04770	0.04735	0.04756	0.04756	0.04756
3	1	0.05897	0.05919	0.05919	0.05864	0.05897	0.05897	0.05897

Table 2

Clamped/simply supported plate: the eigenfrequencies Ω_{mn} for approximate theories: Eringen, Sargsyan, $N=3$, $N=5$, $N=7$, $N=9$ and $N=33$.

m	n	Eringen	Sargsyan	$N=3$	$N=5$	$N=7$	$N=9$	$N=33$
1	1	0.01782	0.01770	0.01756	0.01763	0.01764	0.01765	0.01767
1	2	0.03335	0.03320	0.03293	0.03308	0.03309	0.03310	0.03312
2	1	0.04201	0.04151	0.04094	0.04125	0.04128	0.04130	0.04136
2	2	0.05673	0.05615	0.05532	0.05578	0.05581	0.05584	0.05589
3	1	0.07651	0.07530	0.07373	0.07460	0.07467	0.07471	0.07483
1	3	0.06118	0.06102	0.06035	0.06074	0.06075	0.06075	0.06077

For the third antisymmetric mode, the computed fields are presented in Figs. 5–8. Displacements are shown in Fig. 5, micro-rotation in Fig. 6(a) and stresses and couple stresses in the remaining figures. Generally, all the presented theories produce inferior approximations for the third mode compared to the first mode. Especially the lowest order theories $N=3$, Eringen and Sargsyan render less accurate results, although the $N=3$ theory is generally superior compared to the other two lower order theories. The highest order theory presented, $N=7$, models the fields very accurately. For the displacement in x -direction the Eringen and Sargsyan theories render linear distributions and for the displacement in z -direction these two theories give constant distributions. In contrast, the present theories render results similar to the exact solution, although the accuracy differs among different truncations. This effect is more pronounced for the micro-rotation, stresses and couple stresses. In Fig. 6(a) the micro-rotation for both Eringen’s and Sargsyan’s theories is equal and smaller than the exact theory, contrary to the $N=3$ theory that produces values larger than the exact solution. This behavior is also true for the couple stress m_{12} in Fig. 6(b) which is solely dependent on the micro-rotation ϕ_2 . For the other stresses and couple stress m_{32} a similar behavior is seen, where the approximate theories due to Eringen and Sargsyan produce linear, constant or non-existent results. Note that the stresses t_{33} in Fig. 7(b), t_{31} in Fig. 8(a) and the couple stress m_{32} in Fig. 8 for the present theory fulfill the stated boundary condition at $z=h$, contrary to the theories of Eringen and Sargsyan.

6.3. Eigenfrequencies

In this section, eigenfrequencies for a square plate, $a/h = b/h = 20$ are calculated. The normalized eigenfrequencies for each mode are denoted Ω_{mn} , where m and n refer to the mode numbers in the x and y directions, respectively. The studied cases include a simply supported plate, and two cases where two opposite edges are simply supported while the other are either clamped or free. The edges in y -direction are simply supported for all cases.

Firstly, consider the simply supported case. Here it is possible to obtain exact analytical results, which are used as a benchmark for the approximate theories. Table 1 presents the eigenfrequencies for various modes. It is clear that the approximate theories due to Eringen, Sargsyan and the present $N=3$ theory render reasonably accurate results, even though the results for the $N=3$ theory are slightly less accurate. As expected, the accuracies for all these approximate theories decrease as the mode numbers increase. For higher truncation orders, the results for the present theory converge rapidly to the exact eigenfrequencies. Note also that for a simply supported plate $\Omega_{mn} = \Omega_{nm}$.

Table 3
Free/simply supported plate: the eigenfrequencies Ω_{mn} for approximate theories: Eringen, Sargsyan, $N=3$, $N=5$, $N=7$, $N=9$ and $N=33$.

m	n	Eringen	Sargsyan	$N=3$	$N=5$	$N=7$	$N=9$	$N=33$
1	1	0.006500	0.005936	0.005928	0.005933	0.005933	0.005968	0.005918
1	2	0.02493	0.02377	0.02367	0.02373	0.02373	0.02373	0.02373
2	1	0.01221	0.009757	0.009720	0.009741	0.009742	0.009847	0.009689
2	2	0.03172	0.02819	0.02802	0.02812	0.02812	0.02812	0.02812
3	1	0.02538	0.02215	0.02204	0.02211	0.02211	0.02222	0.02205
1	3	0.05447	0.05274	0.05227	0.05255	0.05255	0.05255	0.05255

Next, consider the case where two opposite edges are simply supported and the other two are clamped. For this case an exact analytical solution cannot be obtained. Therefore a higher order truncation of the present theory, $N=33$, is used as a benchmark solution. Based on the fact that the presented high order eigenfrequencies seem to have converged already at a much lower truncation order, it is assumed that these results coincide with the exact solution. The eigenfrequencies for this case are presented in Table 2. It is noted that the convergence of the present theory is now slower compared to the simply supported plate. Comparing the different theories, it is seen that Sargsyan's theory is generally more accurate than the $N=3$ theory, which in turn is more accurate than Eringen's theory. The Sargsyan theory is slightly less accurate than the $N=5$ theory, especially for the higher modes.

Lastly, consider the case where two opposite edges are simply supported and the other two are free. As before the $N=33$ theory is used as a benchmark and the eigenfrequencies are presented in Table 3. For this case the Eringen's theory renders the least accurate eigenfrequencies while Sargsyan's theory and the $N=3$ theory have approximately equal accuracy. Note that the convergence of modes for the present theory differ to the clamped/simply supported plate, Table 2. Now some modes converge quite fast and other modes initially show a deteriorating convergence effect where the accuracies seem to decrease as the truncation order is increased. The reason for this latter behavior is so far unclear. However, this peculiar effect is only seen for low order truncations. The results are stabilized for higher truncations, where the errors reduce for each truncation step starting from $N=11$.

7. Conclusion

This work presents partial differential plate equations and corresponding edge conditions for an isotropic micropolar plate using a systematic power series expansion approach. Systems of plate equations are developed to arbitrary order for general boundary conditions in a variationally consistent manner. For the lower order approximations, the $N=3$ theory may be regarded as a generalized plate theory of Mindlin type while the $N=5$ theory resembles a generalized plate theory of Reddy type [26]. All orders of plate equations are asymptotically correct to all studied orders. Numerical comparisons for dispersion and cross sectional fields (stress, couple stress, displacement and micro-rotation) are made between the present plate theory of different orders, Eringen's theory, Sargsyan's theory and exact three dimensional theory. Eigenfrequencies are compared between these theories for a simply supported plate, and two plates where two opposing edges are simply supported and the other two are clamped or free. The numerical results illustrate the accuracies of the different approximations. It is seen that the present lower order approximations can be used as refined engineering plate equations when compared to the Eringen and Sargsyan theories. This is particularly the case for the field distributions over the cross section. Higher order approximations may here act as benchmark solutions for simple geometries where the presented numerics indicate that the results for exact theory are obtained.

One important application of the derived set of plate theories is to implement these in finite element codes. Based on the given numerical examples, improved results compared to using traditional plate theories may be obtained from the present lower order approximations in a finite element context. Moreover, it is believed that results similar to what could be calculated adopting three dimensional theory may be obtained in an efficient way by increasing the truncation order within the present theory; at least for not too complicated thin plate geometries in the lower frequency range. Hereby one benefits from the accurate results using one of the present theories, and at the same time the number of elements can be heavily reduced compared to using three dimensional elements.

Another issue is to develop a hierarchy of theories for structures of more complicated material configurations, such as for functionally graded materials. Related work based on power series expansion and recursion relations have previously been carried out on functionally graded [18] and porous [19] plates, and is currently directed towards functionally graded micropolar plates and cylinders.

Appendix A. Plate equations

Here traction free plate equations for the antisymmetric case of order $N=3$ are presented. Using the first sum of Eq. (20) for $l=1, 2$ and the second sum of Eq. (20) for $l=3$ together with Eq. (14) gives for the stresses

$$(\kappa + \mu)u_1^{(1)}(x, y, t) + \mu \partial_x u_3^{(0)}(x, y, t) - \kappa \phi_2^{(0)}(x, y, t)$$

$$+h^2(3(\kappa+\mu)u_1^{(3)}(x,y,t)+\mu\partial_x u_3^{(2)}(x,y,t)-\kappa\phi_2^{(2)}(x,y,t))+\mathcal{O}(h^4)=0, \quad (\text{A.1})$$

$$(\kappa+\mu)u_2^{(1)}(x,y,t)+\mu\partial_y u_3^{(0)}(x,y,t)+\kappa\phi_1^{(0)}(x,y,t) \\ +h^2(3(\kappa+\mu)u_2^{(3)}(x,y,t)+\mu\partial_y u_3^{(2)}(x,y,t)+\kappa\phi_1^{(2)}(x,y,t))+\mathcal{O}(h^4)=0, \quad (\text{A.2})$$

$$\lambda\partial_x u_1^{(1)}(x,y,t)+\lambda\partial_y u_2^{(1)}(x,y,t)+2(\kappa+\lambda+2\mu)u_3^{(2)}(x,y,t) \\ +h^2(\lambda\partial_x u_1^{(3)}(x,y,t)+\lambda\partial_y u_2^{(3)}(x,y,t)+4(\kappa+\lambda+2\mu)u_3^{(4)}(x,y,t))+\mathcal{O}(h^4)=0. \quad (\text{A.3})$$

For the couple stresses using the second sum of Eq. (21) for $l=1, 2$ and the first sum of Eq. (21) for $l=3$ together with Eq. (15), the equations become

$$2\gamma\phi_1^{(2)}(x,y,t)+\beta\partial_x\phi_3^{(1)}(x,y,t) \\ +h^2(4\gamma\phi_1^{(4)}(x,y,t)+\beta\partial_x\phi_3^{(3)}(x,y,t))+\mathcal{O}(h^4)=0, \quad (\text{A.4})$$

$$2\gamma\phi_2^{(2)}(x,y,t)+\beta\partial_y\phi_3^{(1)}(x,y,t) \\ +h^2(4\gamma\phi_2^{(4)}(x,y,t)+\beta\partial_y\phi_3^{(3)}(x,y,t))+\mathcal{O}(h^4)=0, \quad (\text{A.5})$$

$$\alpha\partial_x\phi_1^{(0)}(x,y,t)+\alpha\partial_y\phi_2^{(0)}(x,y,t)+(\alpha+\beta+\gamma)\phi_3^{(1)}(x,y,t) \\ +h^2(\alpha\partial_x\phi_1^{(2)}(x,y,t)+\alpha\partial_y\phi_2^{(2)}(x,y,t)+3(\alpha+\beta+\gamma)\phi_3^{(3)}(x,y,t))+\mathcal{O}(h^4)=0. \quad (\text{A.6})$$

By using the recursion relations, Eqs. (16) and (17), these six plate equations may thus be expressed in terms of the six lowest order expansion functions $\{u_1^{(1)}, u_2^{(1)}, u_3^{(0)}, \phi_1^{(0)}, \phi_2^{(0)}, \phi_3^{(1)}\}$ rendering partial differential equations with respect to x, y and t .

References

- [1] E.F. Cosserat, *Théorie des Corps Déformables*, A. Herman et Fils, Paris, 1906.
- [2] A.C. Eringen, *Microcontinuum Field Theory I. Foundations and Solids*, Springer, New York, 1999.
- [3] J. Altenbach, H. Altenbach, V.A. Eremeyev, On generalized Cosserat-type theories of plates and shells: a short review and bibliography, *Archive of Applied Mechanics* 80 (2010) 73–92.
- [4] A.C. Eringen, Theory of micropolar plates, *Zeitschrift Angewandte Mathematik und Physik* 18 (1967) 12–30.
- [5] A.E. Green, P.M. Naghdi, Micropolar and director theories of plates, *Quarterly Journal of Mechanics and Applied Mathematics* 20 (1967) 183–199.
- [6] F.Y. Wang, On the solutions of Eringen's micropolar plate equations and other approximate equations, *International Journal of Engineering Science* 28 (1990) 919–925.
- [7] S.A. Ambartsumian, The theory of transverse bending of plates with asymmetric elasticity, *Mechanics of Composite Materials* 32 (1996) 30–38.
- [8] H. Altenbach, V.A. Eremeyev, On the linear theory of micropolar plates, *Zeitschrift für Angewandte Mathematik und Mechanik* 89 (2009) 242–256.
- [9] L. Steinberg, Deformation of micropolar plates of moderate thickness, *International Journal of Applied Mathematics* 6 (2011) 1–24.
- [10] S.H. Sargsyan, A.H. Sargsyan, General dynamic theory of micropolar elastic thin plates with free rotation and special features of their natural oscillations, *Acoustical Physics* 57 (2011) 473–481.
- [11] S.H. Sargsyan, A.H. Sargsyan, Dynamic model of micropolar elastic thin plates with independent fields of displacements and rotations, *Journal of Sound and Vibration* 330 (2014) 4354–4375.
- [12] G. del Piero, A rational approach to Cosserat continua, with application to plate and beam theories, *Mechanics Research Communications* 58 (2014) 97–104.
- [13] L. Steinberg, R. Kvasov, Analytical modeling of vibration of micropolar plates, *Applied Mathematics* 6 (2015) 817–836.
- [14] J.D. Achenbach, Free vibrations of a layer of micropolar continuum, *International Journal of Engineering Science* 7 (1969) 1025–1040.
- [15] H.A. Erbay, An asymptotic theory of thin micropolar plates, *International Journal of Engineering Science* 38 (2000) 1497–1516.
- [16] A. Boström, G. Johansson, P. Olsson, On the rational derivation of a hierarchy of dynamic equations for a homogeneous, isotropic, elastic plate, *International Journal of Solids and Structures* 38 (2001) 2487–2501.
- [17] K. Mauritsson, P.D. Folkow, A. Boström, Dynamic equations for a fully anisotropic elastic plate, *Journal of Sound and Vibration* 330 (2011) 2640–2654.
- [18] S.S. Vel, R.C. Batra, Three-dimensional exact solution for the vibration of functionally graded rectangular plates, *Journal of Sound and Vibration* 272 (2004) 703–730.
- [19] P.D. Folkow, M. Johansson, Dynamic equations for fluid-loaded porous plates using approximate boundary conditions, *Journal of the Acoustical Society of America* 125 (2009) 2954–2966.
- [20] A.M. Häggglund, P.D. Folkow, Dynamic cylindrical shell equations by power series expansions, *International Journal of Solids and Structures* 45 (2008) 4509–4522.
- [21] A. Boström, On wave equations for elastic rods, *Zeitschrift für Angewandte Mathematik und Mechanik* 80 (2000) 245–251.
- [22] P.D. Folkow, K. Mauritsson, Dynamic higher-order equations for finite rods, *Quarterly Journal of Mechanics and Applied Mathematics* 63 (2010) 1–22.
- [23] H. Abadikhah, P.D. Folkow, A hierarchy of dynamic equations for solid isotropic circular cylinders, *Wave Motion* 51 (2014) 206–221.
- [24] N.A. Losin, On the equivalence of dispersion relations resulting from Rayleigh–Lamb frequency equation and the operator plate model, *Journal of Vibration and Acoustics* 123 (2001) 417–420.
- [25] A. Kiris, E. Inan, On the identification of microstretch elastic moduli of materials by using data on plates, *International Journal of Engineering Science* 46 (2008) 585–597.
- [26] J.N. Reddy, A refined nonlinear theory of plates with transverse shear deformation, *International Journal of Solids and Structures* 20 (1984) 881–896.